Discriminating the Heavy Jet Production Mechanisms in Associated Z + Heavy Flavor Events at the LHC

S. P. Baranov

Lebedev Physics Institute, Moscow, Russia

A. Bermudez Martinez, H. Jung, S. Taheri Monfared

Deutsches Elektronen-Synchrotron DESY, Hamburg

A. V. Lipatov

Skobeltsyn Institute of Nuclear Physics,
Lomonosov Moscow State University, Russia

and

Joint Institute for Nuclear Research,
Dubna, Moscow, Russia

M. A. Malyshev

Skobeltsyn Institute of Nuclear Physics,
Lomonosov Moscow State University, Russia

Discriminating the heavy jet production mechanisms in associated Z + heavy flavor events at the LHC

S.P. Baranov[1], A. Bermudez Martinez[2], H. Jung[2],
A.V. Lipatov[3,4], M.A. Malyshev[3], S. Taheri Monfared[2]

November 9, 2021

[1]*Lebedev Physics Institute, Moscow, Russia*
[2]*Deutsches Elektronen-Synchrotron DESY, Germany*
[3]*Skobeltsyn Institute of Nuclear Physics, Lomonosov Moscow State University, Moscow, Russia*
[4]*Joint Institute for Nuclear Research, 141980, Dubna, Moscow region, Russia*

Abstract

We reconsider the associated Z boson and charm or beauty jet production at the LHC with paying special attention to the formation dynamics of heavy jets. Two different approaches are studied: first one, where heavy quarks are produced in the hard scattering subprocesses, implemented in the Monte-Carlo generator PEGASUS, and another scenario, where the hard scattering is calculated at NLO with MADGRAPH5_AMC@NLO and TMD parton shower is included (implemented in the Monte-Carlo generator CASCADE3). We compare the predictions obtained in both schemes with latest experimental data for associated $Z + b$ production cross sections and the relative production rate $\sigma(Z+c)/\sigma(Z+b)$ collected by the ATLAS and CMS Collaborations at $\sqrt{s} = 13$ TeV. We introduce two kinematic observables (denoted as z_b and $p_T^{\rm rel}$) which can be used to discriminate the heavy jet production mechanisms. Using these variables we trace the shape of the simulated b-jet events and recommend that these observables be taken into consideration in the forthcoming experimental analyses.

Keywords: Z boson, b-jets, fragmentation, QCD evolution, TMD parton densities.

1 Motivation

With the LHC in operation, one can access a number of 'rare' processes which could have never been systematically studied at previous accelerators. In this article we revisit the associated production of Z bosons and b-jets. This process involves both weak and strong interactions and therefore serves as a complex test of the Standard Model, perturbative QCD and our knowledge of parton densities. On the experimental side, we have at our disposal the data collected by ATLAS and CMS collaborations [1–5].

Earlier, we have demonstrated [6,7] a quite reasonable agreement between the theoretical and experimental results with respect to many observables, such as the differential cross sections and particle correlations. Here we wish to go one step deeper in our understanding and draw attention to two new observables which can be used as clean probes of b-jet formation dynamics. We aim at a difference between 'prompt' and 'non-prompt' production cases. The former class refers to the situation when the b-quark is produced in the hard scattering subprocess; it further radiates lighter partons and after all evolves into a jet containing b-hadrons. The latter class refers to jets initiated by a light parton (gluon or quark), and then b-quarks (or rather b-hadrons) appear from a parton evolution cascade. In principle, one can distinguish between these two kinds of b-jets using an appropriate machine learning technique for gluon-quark jet classification. However, this is not straightforward and should be done carefully [8,9].

We discuss kinematic criteria that can be helpful to discriminate these cases. Namely, we find that in the jets originating from b-quarks (i.e., 'prompt'), b-hadrons carry larger momentum fraction z_b than in other ('non-prompt') jets. Second, in the prompt jets, b-hadrons move closer to the jet axis. The goal of the study is to give quantitative estimates and to see to what extent our expectations are supported by real data.

2 Theoretical framework

There are two commonly used approaches in perturbative QCD (pQCD) calculations for cross sections of processes containing heavy quarks. One of these approaches is the so-called four-flavour number scheme (4FNS), where only gluon distributions and first two quark generations are involved in the QCD evolution equations for parton (quark and gluon) densities in a proton, so that b-quarks appear in a massive final state as a result of gluon splitting $g \to b\bar{b}$. The second approach is the five-flavour number scheme (5FNS), which allows a b-quark density in the initial state where the b-quark is typically treated massless above the flavour threshold. Up to all orders, the 4FNS and 5FNS schemes should give exactly the same results, while at a given order difference can occur[1].

2.1 Calculations with Monte-Carlo generator PEGASUS

To calculate the $Z + b$-jet total and differential cross sections at the LHC we employ two different schemes based on the transverse momentum dependent (TMD) quark and gluon distributions in a proton[2]. The first method was proposed in [6] and relies mainly on the $\mathcal{O}(\alpha\alpha_s^2)$ off-shell gluon-gluon fusion subprocess:

$$g^* + g^* \to Z + b + \bar{b}, \tag{1}$$

---

[1]The discussion on the advantages and disadvantages of the different flavour number schemes can be found, for example, in review [10]. The consistency of both approaches within the context of Parton Branching (PB) approach [11,12] has been recently discussed [13].

[2]For detailed description and discussion of the different approaches involving TMD parton densities see, for example, review [14].

which gives the leading contribution to the production cross section in the small x region, where the gluon density dominates over the quark densities. An essential point here is using the CCFM evolution equation to describe the QCD evolution of the TMD gluon density in a proton. The gauge-invariant off-shell amplitude for the gluon-gluon fusion subprocess has been calculated in Ref. [15, 16], where all the relevant technical details are explained.

In addition, we take into account two subleading subprocesses involving quarks in the initial state. These are the flavor excitation processes

$$q + Q \to Z + Q + q, \tag{2}$$

and the quark-antiquark annihilation processes

$$q + \bar{q} \to Z + Q + \bar{Q}, \tag{3}$$

which could play a role essentially at large transverse momenta (or, respectively, at large x which is needed to produce large p_T events) where the quarks are less suppressed or can even dominate over the gluon density. The contributions from the quark-induced subprocesses (2) and (3) are calculated within a conventional DGLAP-based (collinear) factorization scheme, which provides better theoretical grounds in the region of large x. The evaluation of the production amplitudes is straightforward and needs no explanations.

Our scheme [6, 7] represents a combination of two techniques with each of them being used at the kinematic conditions where it is best suitable. This scheme is implemented in the Monte-Carlo event generator PEGASUS [17], which has been used for numerical calculations. Taking all the three subprocesses (1), (2) and (3) into account we extend the predictions to the whole kinematic range. Note that at least one heavy quark Q is always present in the final state already at the amplitude level.

The parton-level calculation returned by PEGASUS has further been improved by including the effects of the initial and final state parton showering. For the collinear part of the calculation, that has been done using the conventional PYTHIA8 [18] algorithm [3]. The off-shell part of the calculations includes this kind of correction in the form of TMD gluon densities. The subsequent decay $Z \to l^+ l^-$ (including the Z/γ^* interference effects) is incorporated already at the production step at the amplitude level in order to fully reproduce the experimental setup.

For the TMD gluon density in a proton, we used a numerical solution of the CCFM equation [20–23]. We find it to be a suitable option since it smoothly interpolates between the small-x Balitsky-Fadin-Kuraev-Lipatov (BFKL) [24–26] gluon dynamics and large-x DGLAP one. We adopted the latest JH-2013 parametrization, namely, we choose the JH-2013 set 2 [27]. The corresponding TMD gluon density was fitted to high-precision DIS data on the proton structure functions $F_2(x, Q^2)$ and $F_2^c(x, Q^2)$. The fit was based on TMD matrix elements and involves the two-loop strong coupling constant, the kinematic consistency constraint [28, 29] and non-singular terms in the CCFM gluon splitting function [30]. For the conventional quark and gluon densities, we used the MMHT'2014 (NLO) set [31].

2.2 Calculations with Monte-Carlo generator CASCADE3

This method represents a more rigorous scheme based on the parton branching (PB) approach, which was introduced [11, 12] to treat the DGLAP evolution [32–35]. The

---

[3]In fact, we took the TMD parton shower tool implemented into the Monte Carlo event generator CASCADE3 [19] and applied it to the off-shell gluon-gluon fusion subprocess (1).

method provides a solution of these equations and coincides with the standard methods to solve the DGLAP equations for inclusive distributions at NLO and NNLO. It allows one to simultaneously take into account soft-gluon emission at $z \to 1$ and the transverse momentum q_T recoils in the parton branchings along the QCD cascade. The latter leads to a natural determination of the TMD quark and gluon densities in a proton. One of the advantages of this approach is that the PB TMDs can be combined with standard (on-shell) production amplitudes, which can be calculated at higher orders with. Here we use matrix elements calculated with next-to-leading (NLO) order with MAD-GRAPH5_AMC@NLO [36] using the HERWIG6 subtraction terms, which are suitable for combination with PB-TMDs.

The tool to be used to calculate the observables within the PB approach is the Monte-Carlo event generator CASCADE3 [19]. A special procedure is adopted for the initial partons' transverse momenta: a transverse momentum is assigned according to the TMD density, and then the parton-parton system is boosted to its center-of-mass frame and rotated in such a way that only the longitudinal and energy components are nonzero. The energy and longitudinal component of the initial momenta are recalculated taking into account the virtual masses [19, 38]. This method keeps the parton-parton invariant mass exactly conserved, while the rapidity of the partonic system is approximately restored, depending on the transverse momenta.

The PB TMD parton densities were obtained via fitting to precise HERA DIS data. Two sets of them, which differ from each other by the choice of the scale in the QCD coupling, were obtained [39]. In the numerical calculations below we use[4] the PB-NLO-HERAI+II-2018 set 2.

3 Numerical results

Before we turn to the discussion on the 'prompt' and 'non-prompt' b-jets we have to justify our approach by confronting the results of our simulations with the newest CMS and ATLAS data. We start by listing the parameters of our calculations. Following [41], we set the charm and beauty quark masses to $m_c = 1.4$ GeV and $m_b = 4.75$ GeV, the mass of Z boson $m_Z = 91.1876$ GeV, its total decay width $\Gamma_Z = 2.4952$ GeV, and $\sin^2 \theta_W = 0.23122$. The electromagnetic coupling is taken as $\alpha(m_Z) = 1/128.74$.

In the calculations performed with PEGASUS we set $\Lambda_{\text{QCD}}^{(4)} = 200$ MeV and use two-loop QCD coupling according to [27]. The default renormalization scale was taken as $\mu_R^2 = m_Z^2$, while the default factorization scale for the off-shell gluon-gluon fusion subprocess was $\mu_F^2 = \hat{s} + \mathbf{Q}_T^2$, where $\mathbf{Q}_T$ is the net transverse momentum of the initial off-shell gluon pair. This choice is dictated mainly by the CCFM evolution algorithm (see [27] for more information). For the quark-induced subprocesses (2) and (3) we keep it equal to the renormalization scale, $\mu_F = \mu_R$. To estimate the theoretical uncertainties of our PEGASUS calculations for off-shell gluon-gluon fusion subprocess (1) we use auxiliary '+' and '−' TMD gluon densities instead of the default TMD gluon distribution functions. These two sets refer to the varied hard scales in the strong coupling constant α_s in the off-shell amplitude: '+' stands for $2\mu_R$, while '−' refers to $\mu_R/2$ (see [27]). For the quark-induced subprocesses (2) and (3) we just vary the hard scale around its default value between halved and doubled magnitude, as usual.

For the PB calculation with MG5AMC+CA3(Z+1)NLO, we set $m_c = 1.47$ GeV, $m_b = 4.5$ GeV, $\alpha_s(m_Z^2) = 0.118$ and $\mu_R = \mu_F = \frac{1}{2} \sum_i \sqrt{m_i^2 + p_{t,i}^2}$, where the sum runs

---

[4]All the TMD quark and gluon densities in a proton used here are available via the TMDlib tool [40].

4

over all particles and parton in the matrix element. The hard process calculations are performed at NLO with MadGraph5_aMC@NLO [36] with herwig6 subtraction terms and the TMD parton shower is simulated with Cascade3 [19]. The theoretical uncertainties are obtained by varying the scale of the hard process is varied by a factor 2 up and down, provided by MadGraph5_aMC@NLO.

3.1 Z + heavy quark jet production

Now we are in position to present our numerical results. First we discuss $Z + b$ production cross sections measured by the ATLAS Collaboration at $\sqrt{s} = 13$ TeV [5]. The experimental setup was as following: the transverse momenta of the leptons from the Z decay are required to be $p_T^{\text{lead}} > 27$, with pseudorapidities of $|\eta^l| < 2.5$ for muons or $|\eta^l| < 2.47$ for electrons (excluding $1.37 < |\eta^l| < 1.52$). The leptons are isolated from the jets by $\Delta R < 0.4$. The invariant mass of the reconstructed Z-boson has to be within $76 < m^{ll} < 106$. The jets are reconstructed in the anti-k_T algorithm with radius $R_{\text{jet}} = 0.4$ and should have $p_T^{\text{jet}} > 20$ GeV and rapidity $|y| < 2.5$.

Our numerical predictions are shown in Figs. 1 and 2 in comparison with the latest ATLAS data [5]. The shaded bands represent the theoretical uncertainties estimated as described above. In all figures we show predictions (as described above) obtained from MG5aMC+CA3(Z+1)NLO based on a NLO calculation of $Z + 1$ jets with Mad-Graph5_aMC@NLO and TMD parton showers from Cascade3 with and without hadronization, together with predictions obtained from pegasus with and without parton shower.

The MG5aMC+CA3(Z+1)NLO calculations describe well the ATLAS measurements of the Z boson and the b jet rapidity and transverse momenta spectra at low and moderate p_T within the theoretical and experimental uncertainties. From the comparison of MG5-aMC+CA3(Z+1)NLO with and without fragmentation, we estimate the fragmentation correction of $\sim 10\%$ in the larger transverse momentum regions, while at small $p_T(Z)$ and small $p_T(bjet)$ the corrections are significantly larger. These corrections are coming from b-hadrons which are outside the jet with $R = 0.4$. Due to missing higher order contributions in the calculation ($Z + 1$ at NLO) there is a notable underestimation of the data at large transverse momenta, namely $p_T \gtrsim 200$ GeV. These missing higher order contributions lead also to deviations at small $\Delta\phi(Z, b)$, $\Delta R(Z, b)$ and at large $\Delta y(Z, b)$.

The pegasus predictions describe the data quite well within the estimated uncertainties, failing though at large p_T. The scenario implemented into pegasus, where the heavy quark is produced in the hard partonic scattering at the amplitude level, is able to reproduce well the measured distributions in Z boson and b jet rapidity and transverse momenta (at low and moderate p_T). It is interesting to observe, that the distribution of $\Delta\phi(Z, b)$ is well described, even at low $\Delta\phi(Z, b)$, which is in contrast with the PB result. One should however keep in mind that the pegasus calculations do not include fragmentation (unlike the PB ones). Taking into account the fragmentation effect may result in a $\sim 10\%$ drop of cross section [37]. The inclusion of the corresponding fragmentation correction factor could simultaneously result in better agreement by the two approaches. In the $\Delta y(Z, b)$ we observe a similar behavior as for the PB predictions. The final state parton shower effects does not significantly affect the pegasus predictions. It can be easily understood since the main contributions here comes from initial state gluon radiation, which is already taken into account in the CCFM-evolved gluon density.

Now we turn to associated $Z + c$ production at the LHC and discuss the relative production rate $\sigma(Z+c)/\sigma(Z+b)$ as measured by the CMS collaboration at $\sqrt{s} = 13$ TeV [3]. The experimental cuts are: the leading lepton from the Z decay is required to
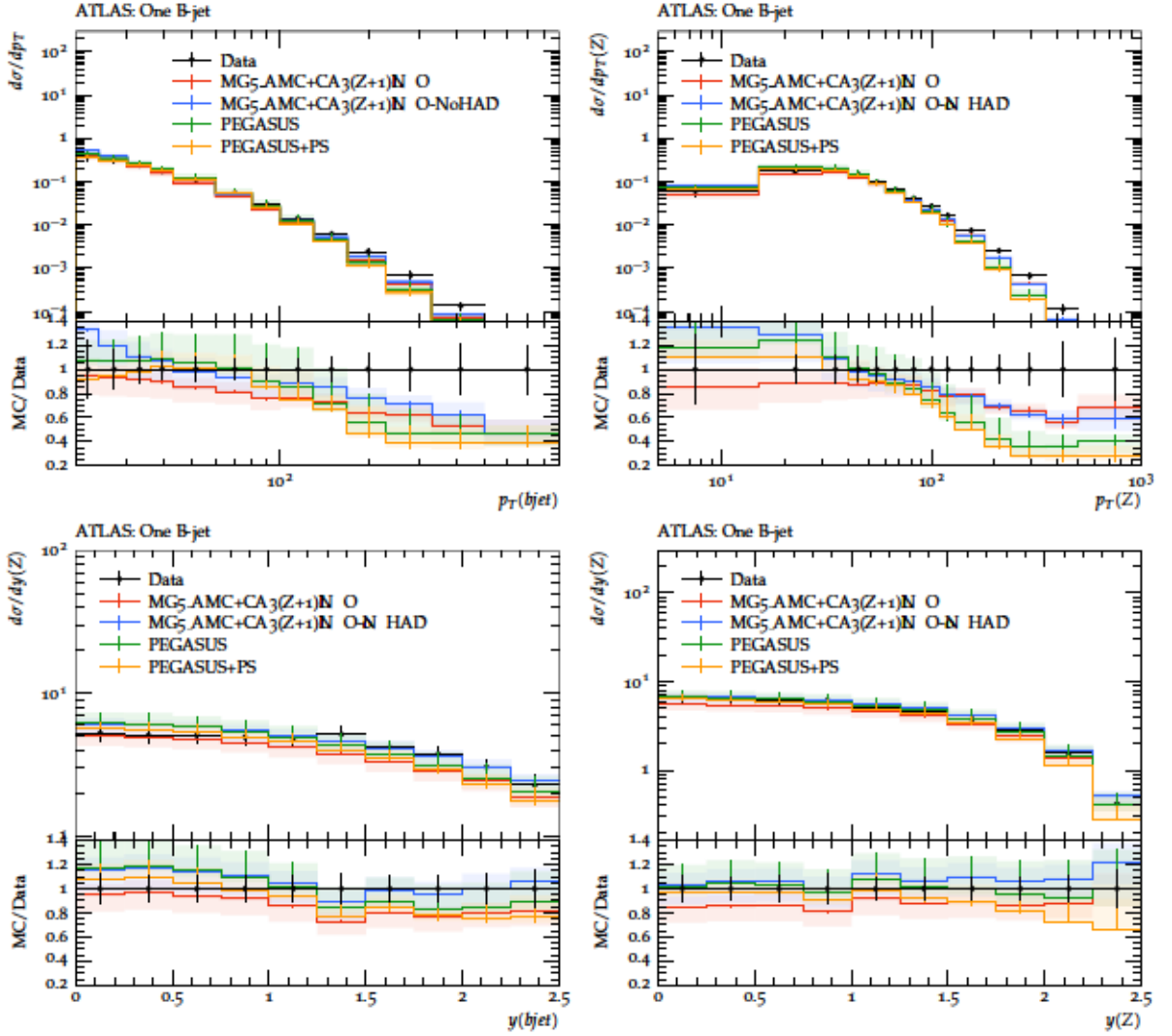
Figure 1: $Z + b$ production differential cross sections as functions of b-jet and Z-boson transverse momenta and rapidities at $\sqrt{s} = 13$ TeV. ATLAS experimental data were taken from [5].

have a transverse momentum $p_T^{\text{lead}} > 26$ GeV, while the subleading lepton must have $p_T^{\text{sublead}} > 10$ GeV; with pseudorapidities within $|\eta^l| < 2.4$ and the dilepton invariant mass should be $71 < m^{ll} < 111$. The leptons are required to be isolated from the jets with $\Delta R < 0.4$. The jets are required to have $p_T^{\text{jet}} > 30$ GeV and $|\eta^{\text{jet}}| < 2.4$, reconstructed with the anti-k_T algorithm with radius $R_{\text{jet}} = 0.4$.

In Fig. 3 we show the results of our calculations for the ratio $\sigma(Z+c)/\sigma(Z+b)$ as a function of Z boson or jet transverse momenta in comparison with the CMS data [3]. The shaded bands represent the estimated uncertainties of our calculations. A good description of the CMS data can be obtained with MG5AMC+CA3(Z+1)NLO The predictions from PEGASUS lie below the data, though being compatible with the data at $\sim 2\sigma$. Thus, despite the fact that both considered scenario provide a more or less reasonable description of inclusive production data (see Figs. 1 and 2), they are very distinct for $\sigma(Z+c)/\sigma(Z+b)$ observables and some correlation variables. The same conclusion was achieved earlier [7] when comparing the PEGASUS and SHERPA (NLO pQCD) predictions, where the same heavy jet production scenario, as in the MG5AMC+CA3(Z+1)NLO is employed. Below we will discuss the kinematic criteria that can be helpful in discriminating these two cases.
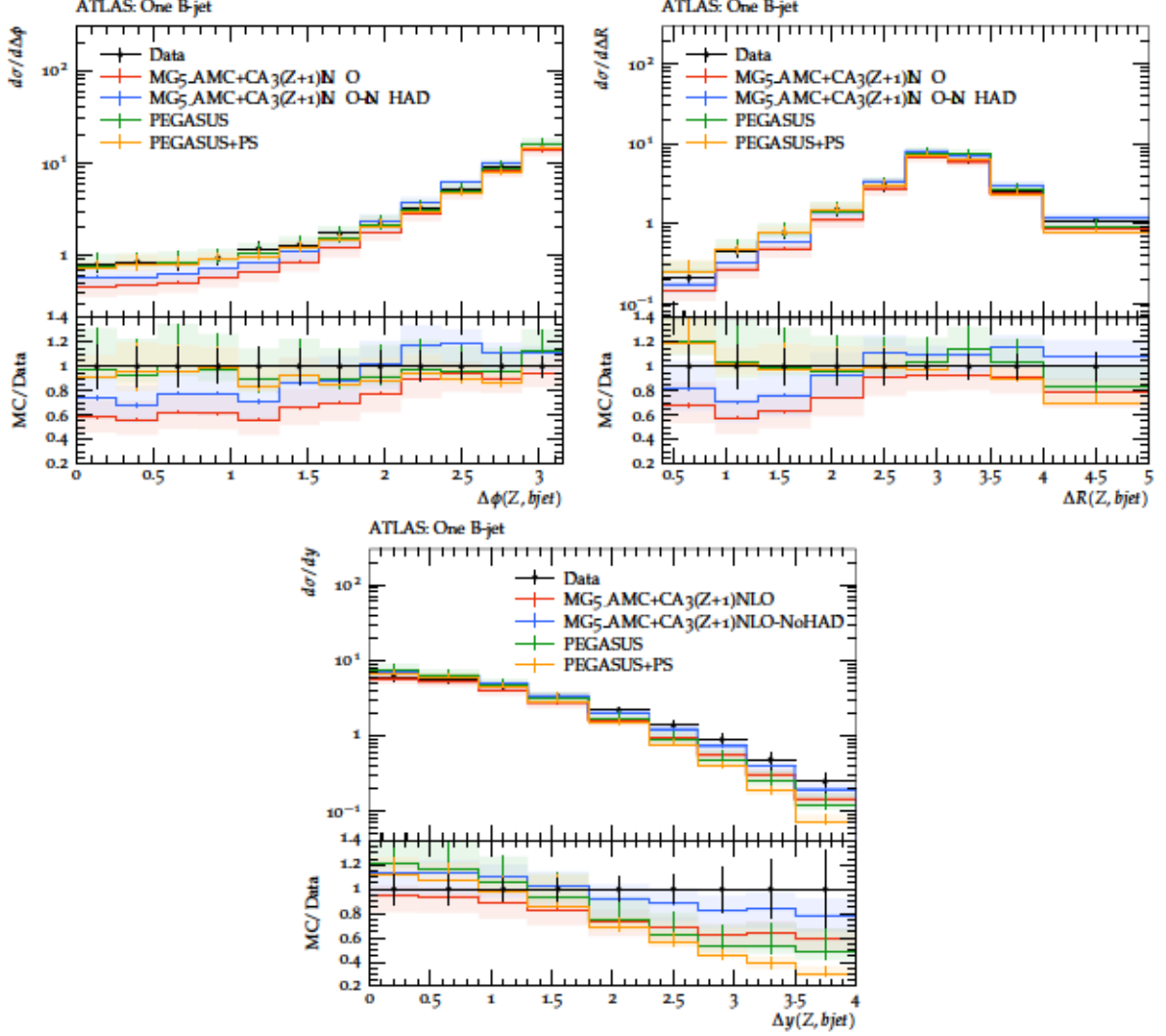
6

Figure 2: $Z + b$ production differential cross sections as functions of the azimuthal angle, angular difference and rapidity differences between b-jet and Z-boson at $\sqrt{s} = 13$ TeV. ATLAS experimental data were taken from [5].
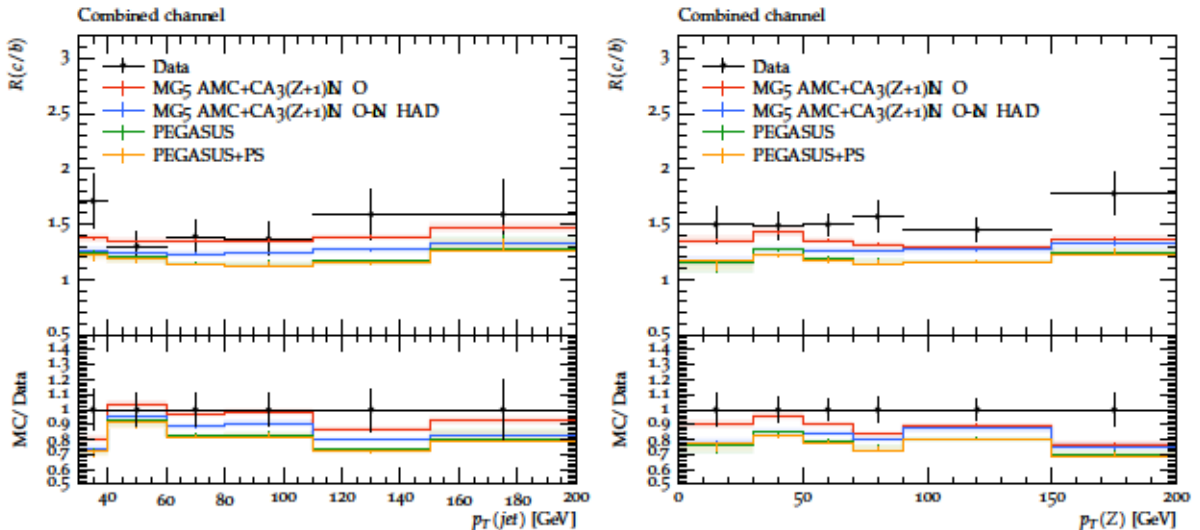
Figure 3: The relative production rate $\sigma(Z + c)/\sigma(Z + b)$ as functions of heavy jet (left panel) and Z-boson (right panel) transverse momentum at $\sqrt{s} = 13$ TeV. The experimental data are from CMS [3].

3.2 Prompt and non-prompt b-jets

Since the two approaches considered above are suitable to describe latest LHC data on $Z + b$ production, we turn to an investigation of observables sensitive to the different sources of heavy jets. Here we concentrate mainly on b-jets, of course, the same arguments can be applied for charmed jets.

In the following we consider kinematic properties of b-jet production by investigating B-hadrons tagged via the semileptonic decay $B \rightarrow \mu + X$: we consider the fractional energy z_b carried by the decay muon with respect to the total b-jet energy and the muon transverse momentum p_T^{rel} with respect to the b-jet axis. With both variables we aim to distinguish between prompt b-production, where the b-quark exists already at the matrix element level, and non-prompt b-production, where the b-quark is generated during the jet evolution. We expect large z_b and small p_T^{rel} (relative to the jet p_T) for prompt b production, while non-prompt b-production would lead to significantly smaller values for z_b and a larger tail for p_T^{rel}.

In Fig. 4 the distribution of z_b and p_T^{rel} are shown for different thresholds of the jet transverse momentum: $p_T^{jets} > 30, 50, 100, 200, 300$ GeV. Jets with larger transverse momenta provide larger phase space for parton radiation cascades. Accordingly, they show a larger fraction of 'non-prompt' B-hadrons resulting in a larger fraction of low-energy muons (muons with low z_b) and in larger fraction of muons with high p_T^{rel} (muons with large deviation from the jet direction).

We find, that the intuitive variables z_b and p_T^{rel} are very powerful to distinguish prompt and non-prompt b production

4 Conclusion

We have considered the production of Z bosons associated with charm and beauty jets at LHC conditions. We investigated two different schemes.

We find that the combination of three basic subprocesses (1) – (3) involving heavy quarks in final states provides a consistent description of Z boson and/or b-jet transverse
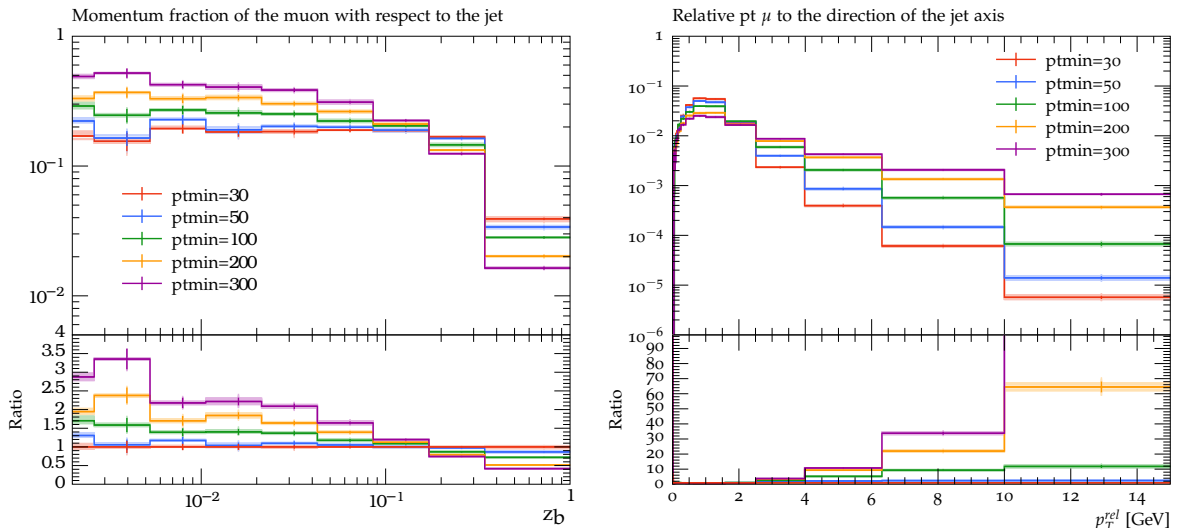
Figure 4: $Z + b$ production differential cross sections as functions of the energy fraction carried by the decay muon with respect to the total b-jet energy and the muon transverse momentum with respect to the b-jet axis at $\sqrt{s} = 13$ TeV for different cuts on the minimal p_T of the jet.

momenta and rapidity distributions as well as different correlation observables in $Z + b$ events at low and moderate p_T. This can be seen from a direct comparison between the model predictions obtained using the Monte-Carlo generator PEGASUS and recent LHC data.

In another approach we consider $Z + jet$ production at NLO, where heavy quarks can be produced directly in the matrix element, or during the showering process. We perform the calculations based on the Parton Branching TMDs together with TMD shower for the initial state cascade. Such calculations were performed using MG5AMC+CA3(Z+1)NLO. We find very good description of the measurement at not too large transverse momentum of the Z boson.

We classify different b-jet production mechanisms as prompt and non-prompt, depending whether the heavy quark is present at matrix element level or generated during the jet evolution.

Events of the prompt and non-prompt types show rather different kinematic properties, that can be seen, in particular, in relative production rate $\sigma(Z+c)/\sigma(Z+b)$ measured very recently by the CMS Collaboration for the first time. The ratio of c over b jet production is also reasonably well described by the PB prediction of MG5AMC+CA3(Z+1)NLO.

Considering the $Z + b$ events as a representative example, we see that jets with larger transverse momenta contain larger fraction of non-prompt b-hadrons, that results in larger fraction of low-energy muons and in larger fraction of muons with large deviation from the jet direction. We recommend that the relevant observables, z_b and p_T^{rel}, be used in the forthcoming experimental analyses.

Acknowledgments

References

[1] CMS Collaboration, JHEP **12**, 039 (2013).

[2] CMS Collaboration, Eur. Phys. J. C **77**, 751 (2017).

[3] CMS Collaboration, Phys. Rev. D **102**, 032007 (2020).

[4] ATLAS Collaboration, JHEP **10**, 141 (2014).

[5] ATLAS Collaboration, JHEP **07**, 044 (2020).

[6] S.P. Baranov, H. Jung, A.V. Lipatov, M.A. Malyshev, Eur. Phys. J. C **77**, 772 (2017).

[7] A.V. Lipatov, G.I. Lykasov, M.A. Malyshev, A.A. Prokhorov, S.M. Turchikhin, Phys. Rev. D **97**, 114019 (2018).

[8] J. Pumplin, Phys. Rev. D **44**, 2025 (1991).

[9] A. Romero, D. Whiteson, M. Fenton, J. Collado, P. Balsi, arXiv:2103.09103 [hep-ph].

[10] F. Maltoni, G. Ridolfi, M. Ubiali, JHEP **07**, 022 (2012).

[11] F. Hautmann, H. Jung, A. Lelek, V. Radescu, R. Zlebcik, Phys. Lett. B **772**, 446 (2017).

[12] F. Hautmann, H. Jung, A. Lelek, V. Radescu, R. Zlebcik, JHEP **01**, 070 (2018).

[13] H. Jung, S. Taheri Monfared, arXiv:2106.09791 [hep-ph].

[14] R. Angeles-Martinez et al., Acta Phys. Polon. **46**, 2501 (2015).

[15] S.P. Baranov, A.V. Lipatov, N.P. Zotov, Phys. Rev. D **78**, 014025 (2008).

[16] M. Deak, F. Schwennsen, JHEP **09**, 035 (2008).

[17] A.V. Lipatov, M.A. Malyshev, S.P. Baranov, Eur. Phys. J. C **80**, 330 (2020).

[18] T. Sjöstrand et al., Comput. Phys. Commun. **191**, 159 (2015).

[19] S. Baranov et al. Eur. Phys. J. C **81**, 425 (2021).

[20] M. Ciafaloni, Nucl. Phys. B **296**, 49 (1988).

[21] S. Catani, F. Fiorani, G. Marchesini, Phys. Lett. B **234**, 339 (1990).

[22] S. Catani, F. Fiorani, G. Marchesini, Nucl. Phys. B **336**, 18 (1990).

[23] G. Marchesini, Nucl. Phys. B **445**, 49 (1995).

[24] E.A. Kuraev, L.N. Lipatov, V.S. Fadin, Sov. Phys. JETP **44**, 443 (1976).

[25] E.A. Kuraev, L.N. Lipatov, V.S. Fadin, Sov. Phys. JETP **45**, 199 (1977).

[26] I.I. Balitsky, L.N. Lipatov, Sov. J. Nucl. Phys. **28**, 822 (1978).

[27] F. Hautmann, H. Jung, Nucl. Phys. B **883**, 1 (2014).

[28] J. Kwiecinski, A.D. Martin, P. Sutton, Z. Phys. C **71**, 585 (1996).

[29] B. Andersson, G. Gustafson, J. Samuelsson, Nucl. Phys. B **467**, 443 (1996).

[30] M. Hansson, H. Jung, arXiv:hep-ph/0309009.

[31] L.A. Harland-Lang, A.D. Martin, P. Motylinsky, R.S. Thorne, Eur. Phys. J. C **75**, 204 (2015).

[32] V.N. Gribov, L.N. Lipatov, Sov. J. Nucl. Phys. **15**, 438 (1972).

[33] L.N. Lipatov, Sov. J. Nucl. Phys. **20**, 94 (1975).

[34] G. Altarelli, G. Parisi, Nucl. Phys. B **126**, 298 (1977).

[35] Yu.L. Dokshitzer, Sov. Phys. JETP **46**, 641 (1977).

[36] J. Alwall et al., JHEP **07**, 079 (2014).

[37] ATLAS Collaboration, Phys. Lett. B **706**, 295 (2012).

[38] M. Bengtsson, T. Sjostrand, M. van Zijl, Z. Phys. C **32**, 67 (1986).

[39] A. Bermudez Martinez et al. Phys. Rev. D **99**, 074008 (2019).

[40] N.A. Abdulov et al. Eur. Phys. J. C **81**, 752 (2021).

[41] Particle Data Group, PTEP **2020**, 083C01 (2020).